frontiers in Physics

ORIGINAL RESEARCH
published: 10 January 2020
doi: 10.3389/fphy.2019.00223

Transcranial Magnetic Resonance Imaging-Guided Focused Ultrasound Treatment at 1.5 T: A Retrospective Study on Treatment- and Patient-Related Parameters Obtained From 52 Procedures

Cesare Gagliardo[1†], Maurizio Marrale[2,3†], Costanza D'Angelo[1], Roberto Cannella[1], Giorgio Collura[1,2,3], Gerardo Iacopino[4], Marco D'Amelio[5], Alessandro Napoli[6], Tommaso Vincenzo Bartolotta[1], Carlo Catalano[6], Roberto Lagalla[1] and Massimo Midiri[1]*

[1] Section of Radiological Sciences, Department of Biomedicine, Neuroscience and Advanced Diagnostics, University of Palermo, Palermo, Italy, [2] Department of Physics and Chemistry, University of Palermo, Palermo, Italy, [3] National Institute of Nuclear Physics, Section of Catania, Catania, Italy, [4] Section of Neurosurgery, Department of Biomedicine, Neuroscience and Advanced Diagnostics, University of Palermo, Palermo, Italy, [5] Section of Neurology, Department of Biomedicine, Neuroscience and Advanced Diagnostics, Palermo, Italy, [6] Radiology Section, Department of Radiological, Oncological and Anatomopathological Sciences, "Sapienza" University of Rome, Rome, Italy

OPEN ACCESS

Edited by:
Nicola Toschi,
University of Rome Tor Vergata, Italy

Reviewed by:
Sigrun Roat,
Medical University of Vienna, Austria
Beat Werner,
University of Zurich, Switzerland

***Correspondence:**
Cesare Gagliardo
cesare.gagliardo@unipa.it

[†]These authors have contributed equally to this work

Specialty section:
This article was submitted to Medical Physics and Imaging, a section of the journal Frontiers in Physics

Received: 16 August 2019
Accepted: 02 December 2019
Published: 10 January 2020

Citation:
Gagliardo C, Marrale M, D'Angelo C, Cannella R, Collura G, Iacopino G, D'Amelio M, Napoli A, Bartolotta TV, Catalano C, Lagalla R and Midiri M (2020) Transcranial Magnetic Resonance Imaging-Guided Focused Ultrasound Treatment at 1.5 T: A Retrospective Study on Treatment- and Patient-Related Parameters Obtained From 52 Procedures. Front. Phys. 7:223. doi: 10.3389/fphy.2019.00223

Objective: To present a retrospective analysis of patient- and sonication-related parameters of a group of patients treated with a transcranial magnetic resonance imaging (MRI)-guided focused ultrasound (tcMRgFUS) system integrated with a 1.5-T MRI unit.

Methods: The data obtained from 59 patients, who underwent the tcMRgFUS procedure from January 2015 to April 2019, were retrospectively reviewed for this study. The following data, among others, were mainly collected: skull density ratio (SDR), skull area (SA), number of available transducer elements (Tx), and estimated focal power at target (FP). For each of the four different treatment stages, we calculated the number of sonication processes (S_n), user-defined sonication power (S_p), effective measured power (S_{mp}), sonication duration (S_d), user-defined energy (E), effective measured energy (E_m), maximum temperature (T_{max}), and MR thermometry plane orientation. Furthermore, the time delay between each sonication (S_t) and the total treatment time (T_t) were recorded.

Results: Fifty-two patients (40 males and 12 females; age 64.51 ± SD 11.90 years; range 26–86 years), who underwent unilateral Vim thalamotomy (left = 50, 96.15%; right = 2, 3.85%) for medication-refractory essential tremor ($n = 39$; 78%) or Parkinson tremor ($n = 13$; 22%) were considered. A total of 1,068 (95.10%) sonication processes were included in our final analysis (average S_n per treatment: 20.65 ± 6.18; range 13–41). The energy released onto the planned target was found to decrease with the SDR for all temperature ranges. A positive correlation was observed between the slope of T_{max} vs. E_m plot and the SDR ($R^2 = 0.765$; $p < 0.001$). In addition, the T_{max} was positively correlated with SDR ($R^2 = 0.398$; $p < 0.005$). On the contrary, no significant correlation was found between SDR and SA or Tx. An analysis of the MR thermometry scanning

plane indicated that, at our site, the axial and the coronal planes were used (on average) 10.4 (SD ± 3.8) and 7.7 (SD ± 3.0) times, respectively, whereas the sagittal plane was used only 2.5 (SD ± 3.0) times per treatment.

Conclusion: Our results confirm the factors that significantly influence the course of a tcMRgFUS procedure even when a 1.5-T MRI scanner is used for procedure guidance. The experience we gained in this study indicates that the SDR remains one of the most significant technical parameters to be considered in a tcMRgFUS procedure. The possibility of prospectively setting the sonication energy according to the presented curves of energy delivery as a function of SDR for each treatment stage could provide a further understanding and a greater awareness of this emerging technology.

Keywords: high-intensity focused ultrasound ablation, interventional magnetic resonance imaging, stereotaxic techniques, essential tremor, Parkinson's disease

INTRODUCTION

Magnetic resonance imaging-guided focused ultrasound (MRgFUS) is a non-invasive thermal ablation method that involves high-intensity FUS energy and MRI for anatomical imaging and real-time thermal mapping [1]. Thanks to novel technology, it is now possible to create a sharp focal point in the planned target through an intact skull for the treatment of neurological disorders [transcranial MRgFUS (tcMRgFUS)] [2]. As a result, a major feat has been achieved in the field of therapeutic brain lesioning, which was previously partially abandoned over the years and increasingly replaced by deep brain stimulation (DBS) since its introduction in the late 1980s [3]. Radio-frequency stereotactic ablation is invasive (skin and skull incisions) and involves a few risks (infections, hemorrhage, imprecise targeting) [4]. Stereotactic radiosurgery, although non-invasive, utilizes ionizing radiations; furthermore, targeting is performed only using atlas coordinates, and the physicians cannot anticipate the clinical results because the radiobiological effects occur delayed and are not always predictable [4]. Although DBS is invasive and involves procedure-related risks, possible hardware malfunction, and requires battery replacement that may discourage patients [3, 5], it has been widely employed in the past few years because it introduced the prospect of neuromodulation. On the contrary, the tcMRgFUS method does not use ionizing radiation and is non-invasive; in addition, patient feedback allows the physician to optimize the target before a permanent lesion is made because its clinical effects can be evaluated immediately. Clinical results of tcMRgFUS systems integrated with 3-T MRI units have already been reported for patients with essential tremor (ET) [6], Parkinson's disease (PD) [7–9], neuropathic pain [10], and psychiatric disorders [11]; these results have indicated the possibility of a wide range of experimental applications [12–14]. In recent years, because of the use of a dedicated surface coil, which allows considerable gain in terms of signal-to-noise ratio [15], the tcMRgFUS procedure has been performed with MRI units operating at 1.5 T [16]. Although numerous studies have been conducted on this subject, most studies are focused only on the clinical aspects, and some technical limits thus remain to be investigated. In 2015, Chang et al. [17] studied the correlation between the skull-related factors and the maximal area temperature using samples obtained from 25 patients who were treated with a tcMRgFUS system integrated with a 3-T unit. More recently, D'Souza et al. [18] investigated the influence of skull bone characteristics on the efficacy and safety of FUS procedure; furthermore, Boutet et al. [19] studied the significance of skull bone characteristics in selecting candidates for the procedure. Furthermore, Jung et al. [20] investigated the technical limitations of the acoustic properties of skull (five non-embalmed cadaver skulls and 46 patients who underwent the tcMRgFUS procedure) to identify the skull density ratio (SDR), skull volume, and incidence angle of acoustic rays against the skull surface as the important factors to establish a successful procedure.

Accordingly, we present a retrospective analysis on the dependence of treatment-related parameters on patient-related features for a series of patients who were treated with a tcMRgFUS system integrated with a 1.5-T MRI unit.

MATERIALS AND METHODS

The institutional review board approved this study, and all of the patients signed an informed consent for this study in accordance with the Declaration of Helsinki. The data obtained from 59 patients who underwent the tcMRgFUS procedure at our university hospital from January 2015 to April 2019 were retrospectively reviewed for this study.

The ExAblate 4000 (InSightec Ltd, Haifa, Israel) integrated with a Signa HDxt 1.5-T MRI unit (GE Medical Systems, Milwaukee, Wisconsin, USA) is the tcMRgFUS system available in our facility.

Only the patients who underwent the tcMRgFUS procedure with a clearly visible lesion in intraoperative imaging were selected for this study. Intraoperative imaging was realized using a dedicated two-channel coil embedded into an elastic membrane that is placed on the patient's head and fixed to the transducer to achieve a watertight seal [15]. Furthermore, we used an axial 2-D T2-weighted (T2w) fast recalled fast spin-echo (FRFSE) pulse sequence as the MRI sequence to identify thalamic lesions. This

MRI sequence has been scanned based on the requirements of the treating physician, among high-energy sonications, and for final lesion assessment at the end of the procedure just before water drainage from the helmet and discharging the patient from the treating table. The scan parameters were as follows: slice thickness 2 mm; no gap; TR 4,461 ms; TE 103 ms; ETL 19; FOV 22 cm^2 × 22 cm^2; matrix 384 × 288; NEX 2; number of slices 19 (AC-PC alignment, basal ganglia region coverage).

For each patient, the SDR and the skull area (SA) exposed to the transducer were calculated using the ExAblate workstation, from the screening head CT scan obtained approximately 3 months prior to the treatment using a 16-row multidetector CT scanner (BrightSpeed, GE Medical Systems, Milwaukee, Wisconsin, USA). The CT scan parameters were as follows: tube voltage 120 kV, tube current 220 mA, pure axial plane (0° gantry tilting), sequential acquisition, slice thickness 1.25 mm, and bone kernel (GE bone plus, WL 600/WW 2500).

The ExAblate workstation calculates the SDR score by dividing the skull CT dataset into small samples and calculating the average of the ratio between the trabecular and the cortex bone CT values (in Hounsfield units) for all voxels of the samples [17]. Therefore, a homogeneously compact skull (i.e., trabecular layer is negligible) has an SDR score of 1, whereas a skull characterized by a highly represented trabecular layer has a smaller SDR score (closer to 0). Knowledge of this score is mandatory to apply a phase correction algorithm [2] that enables the tcMRgFUS system to achieve a coherent summation of sufficient energy delivery to the planned target *via* a compensation of the different speeds of the US beam through bone to that of the soft tissues, along with the variability in skull thickness and incidence angle of acoustic rays against the skull surface [17, 21].

The SA was calculated during the treatment simulations (SA_s) (by accordingly planning the target and the transducer location) and the actual treatment (SA_t) using the ExAblate workstation.

Each treatment was titrated by sonication (in steps of small energy increments) to first verify the alignment of the thermal spot in all three axes and then perform treatment retargeting based on real-time feedback from patients prior to actual lesioning. Furthermore, the temperatures were calculated using the ExAblate software by real-time MR thermometry based on proton resonance frequency (PRF) shift of water molecules by considering a baseline temperature of 37°C (MR thermometry sequence parameters: gradient echo pulse sequence, TR 26.172 ms, TE 12.996 ms, FA 30, slice thickness 3 mm, FOV 28 cm^2 × 28 cm^2, matrix 256 × 128, bandwidth 43.4375 Hz/pixel, temporal resolution 3.5 s). Four different typical consecutive treatment stages, each characterized by a maximum temperature (T_{max}) limit at the target area, were considered: stage I: thermal spot alignment ($T_{max} \leq 45°C$); stage II: real-time clinical evaluation prior to actual lesioning ($45°C < T_{max} \leq 50°C$); stage III: permanent lesioning with low power ($50°C < T_{max} \leq 55°C$); stage IV: lesion consolidation with high power ($T_{max} > 55°C$). For each treatment, the following treatment-related parameters were collected: number of sonication processes (S_n), user-defined sonication power (S_p), effective measured power (S_{mp}), sonication duration (S_d), user-defined energy (E), effective measured energy (E_m), maximum temperature (T_{max}), and MR thermometry plane orientation (Ax, axial; Cor, coronal; Sag, sagittal).

All of the sonication-related parameters were calculated for the abovementioned treatment stages. If no significant amount of energy was achieved ($S_{mp} \leq 50\%$ of S_p and $E_m \leq 50\%$ of E), the sonication was defined as inconsistent. All sonication processes, aborted by the patient, by the treating (or the monitoring) physician before a significant amount of energy was released ($S_{mp} \leq 50\%$ of S_p and $E_m \leq 50\%$ of E), or because of any technical failure and device malfunction, were considered inconsistent and were thus excluded from the statistical analysis.

All patient-related parameters were calculated during the simulations and the actual treatments after marking as no pass regions sensible structures (i.e., frontal sinuses, intracranial calcifications, skin defects as scars or nevi) and elastic membrane folding (for treatment sessions only). Furthermore, the following parameters were considered: number of transducer elements (Tx_s for simulations and Tx_t for actual treatment) and estimated focal power at the target (FP_s for simulations and FP_t for actual treatment). In addition, the time delay between each sonication (S_t) and the duration of the entire procedure (treatment time: T_t) (considering the time elapsed from the first to the last sonication) were recorded. Patients with SDR ≤ 0.3, and/or SA < 250 cm^2, and/or Tx_s elements < 700 at our university hospital were excluded from this study after performing treatment simulations and did not undergo the tcMRgFUS procedure.

The correlations between the abovementioned parameters were calculated, along with the corresponding *p*-values using the Pearson formula.

The programs, which were developed on an *ad hoc* basis, used in this study were written in Python language using the package for Scientific computing (SciPy) [22] within the framework of SageMath [23]. This software automatically reads the output files produced by the ExAblate workstation, evaluates the average values for the various parameters considered, estimates the correlations between these parameters, and generates output plots. The main advantage of this software is that, once implemented, it could automatically analyze an arbitrary number of datasets of patients from different sites (if available).

RESULTS

Of the total number of 59 patients, only the data of 52 tcMRgFUS procedures were considered in this study because two procedures were aborted, four failed, and the data of a successful bilateral central lateral thalamotomy procedure were excluded (see **Table S1**). No patient was excluded because of low SDR and/or SA and/or Tx_s elements. The demographic data (sex, age, and disease) and patient- (thalamotomy side, SDR, SA, Tx, and FP) and treatment-related (S_n and T_t) parameters are provided in **Table 1**.

A total of 1,123 sonication processes were performed in our retrospective analysis. Furthermore, 55 sonication processes (4.90%) were considered inconsistent, and the data of the remaining 1,068 sonication processes (95.10%) were

TABLE 1 | Summary of patient demographics and treatment data included in the final analysis.

Characteristics	Number
Patients	52
Gender	
Males	40 (76.92%)
Females	12 (23.08%)
Age	
Mean ± SD	64.51 ± 11.90
Range	26–86
Tremor etiology	
Essential tremor	39 (78%)
Parkinson tremor*	13 (22%)
Thalamotomy side	
Left Vim	50 (96.15%)
Right Vim	2 (3.85%)
Skull density ratio—SDR	
Mean ± SD	0.51 ± 0.10
Range	0.34–0.74
Skull Area—SA_s (SA_t)	
Mean ± SD	359 (344) ± 25.3 (27.5)
Range	289–406 (293–410)
Number of transducer elements—Tx_s (Tx_t)	
Mean ± SD	959 (927.5) ± 24.6 (50.61)
Range	880–998 (799–1,000)
Focal Power—FP_s (FP_t)	
Mean ± SD	12 (13.3) ± 7.73 (12.8)
Range	2–51(4-68)
Number of sonication processes—S_n (stage I—alignment)	
Mean ± SD	3.25 ± 2.06
Range	3–9
Number of sonication processes—S_n (stage II—verification)	
Mean ± SD	6.60 ± 3.60
Range	1–18
Number of sonication processes—S_n (stage III—treat low)	
Mean ± SD	6.48 ± 3.52
Range	1–17
Number of sonication processes—S_n (stage IV—treat high)	
Mean ± SD	4.21 ± 3.34
Range	0–14
Treatment time (T_t)	
Mean ± SD	2 h 17 m ± 45 m
Range	1 h 12 m–3 h 58 m

*Age is expressed in years, SA in square centimeters, Tx as the number of available elements, and FP in watts. *A patient with both tremor and Parkinsonism, who underwent the tcMRgFUS Vim ablation procedure in 6 months after the first treatment, has been included in this group [24].*

included in the final analysis (with an average sonication number per treatment of 20.65 ± 6.18; range 13–41). The number of sonication processes per treatment stage averaged over patients (with related standard deviation and range) is provided in **Table 1**. Furthermore, the summary of the sonication parameters for each treatment stage is reported in **Table 2**.

Moreover, the dependence of the energy released onto the planned target as a function of the SDR was considered. Specifically, the effective E_m (calculated by the ExAblate workstation) averaged over patients and sonication processes was calculated for the four treatment stages. The total SDR range was subdivided, as shown in **Figure 1**. For all temperature ranges, E_m decreases with SDR, confirming the results of research and clinical practice established already over the years by facilities performing this procedure using the tcMRgFUS system integrated with a 3-T MRI unit. Therefore, if a patient has a high SDR value, only low-energy delivery is usually required to achieve a given temperature, relative to patients with low SDR values. In **Figure 1**, the solid lines represent the best fit curves with power-law function (more information, including the best fit parameters, is reported in **Supplementary Material**), and the dashed lines represent the spline curves that connect the experimental data. The spline curves are shown to indicate the point fluctuations observed on these average values.

Moreover, for each patient, the trend of temperature rise with E_m was analyzed. **Figure 2** shows this trend for three patients with different SDR values (0.37, 0.51, and 0.71). It was found that a higher energy is required in case of patients with low SDR values to achieve the desired temperature rise because the skull hampers the HIFU energy transmission by reflecting and attenuating energy at interfaces differently compared with the case of patients with high SDR values. Thus, the amount of energy required to reach a temperature of 50°C at the target in the case patients with an SDR of 0.37 and 0.51 was more than five and two times, respectively, higher than that required for a patient with an SDR = 0.71. In the case of a patient with SDR = 0.37, as shown in **Figure 2**, even if five sonication processes were performed with increasing energies (E_m range 34–36 kJ), realizing a temperature rise beyond 50°C was impossible (temperature at the target previously achieved a more bearable 27 kJ sonication, confirming that the temperature rise is not always proportional to the increase in sonication power). Furthermore, the steeper the increase in temperature (i.e., steep slope), the smaller the total amount of energy delivered at each treatment stage. Thus, the slope describes the ease with which temperature can be increased by HIFU exposure in relation to SDR.

Therefore, the slope of the best fit curve was calculated for each patient and plotted as a function of SDR. The results of this analysis are illustrated in **Figure 3**, which clearly indicate that a correlation exists between the slope of the temperature vs. energy plot and the SDR ($R^2 = 0.765$; $p < 0.001$). Therefore, when treating a patient with a low SDR value, the physician could face difficulties in locally increasing the temperature that could lead to suboptimal lesioning and/or longer treatment duration (the higher the energy released, the longer the system cooling time). On the contrary, in patients with high SDR values, the HIFU beam transmission across the skull is less hampered, and attaining the ablation temperature is thus generally not difficult even with a low energy delivery.

Figure 4 shows the peak temperature achieved as a function of SDR. The correlation is significantly positive ($R^2 = 0.398$; $p < 0.005$) and further indicates that increasing the temperature in patients with high SDR values is more feasible. However,

TABLE 2 | Summary of sonication parameters for each treatment stage for all considered patients.

Treatment stage	Temperature (°C)		Power (W)	Measured power (W)	Actual power %	S_n (s)	Energy (J)	Measured energy (J)	Actual energy %	T_{max} (°C)	SD of T_{max} (°C)
Alignment (I)	$T < 45$	mean	316.15	302.49	95.68	11.43	3,610.14	2,360.17	65.38*	42.89	1.90
Verify (II)	$45 \leq T < 50$	mean	413.70	399.22	96.50	13.55	5,238.45	4,899.29	93.53	47.58	1.41
Treat low (III)	$50 \leq T < 55$	mean	642.87	614.59	95.60	17.36	10,034.22	9,326.26	92.94	52.41	1.45
Treat high (IV)	$T \geq 55$	mean	800.14	761.54	95.18	16.84	11,560.96	10,799.17	93.41	57.98	2.55
		max	1,300.00	1,218.70	95.68	80.00	39,000.00	36,323.20	93.14	67.93	n.a.

**If releasing a high percentage of planned energy during alignment sonication processes was not possible, the acoustic threshold was increased from the ExAblate workstation (identified by the vendor as "tissue type level 1" option). Thus, in our analysis, the mean actual energy percentage was lower than that for other treatment stages, even by neglecting inconsistent sonication processes.*

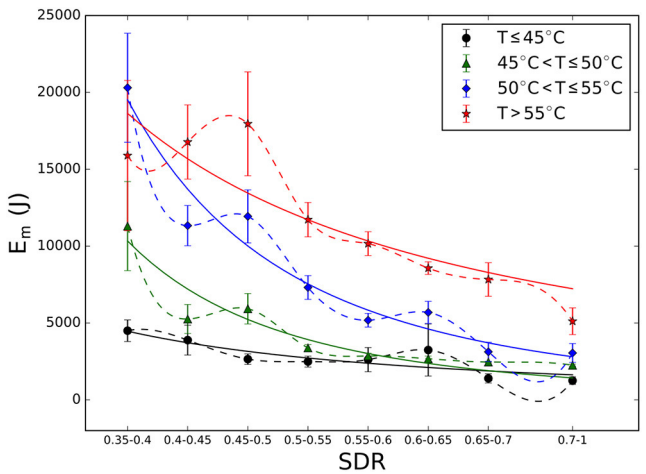

FIGURE 1 | Energy released on the target for various skull density ratio (SDR) values in the four treatment stages (and related temperature ranges). Dashed lines represent spline curves that connect the experimental data, and continuous lines represent the best fit curves (more information is provided in **Table S2**). For low SDR range (0.35–0.4), the measured energy values for the treatment stage III are higher than those for treatment stage IV because we were unable to achieve an increase in temperature of above 55°C in six patients, even by increasing the planned energy.

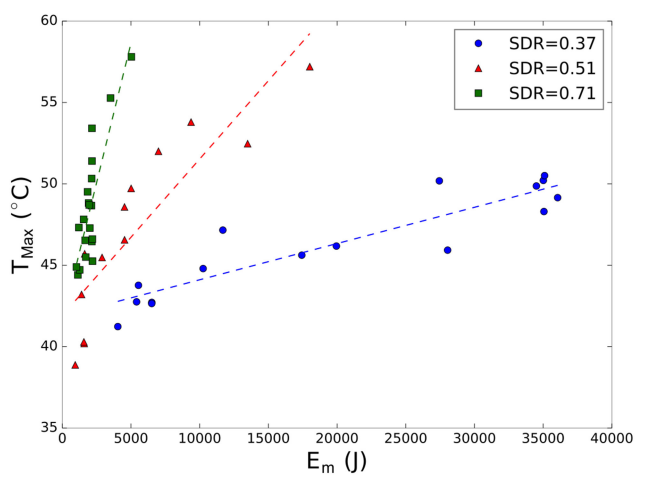

FIGURE 2 | Maximum peak temperature (Tmax) as a function of measured energy (Em) for three patients with different skull density ratio (SDR) values (blue 0.37; red 0.51; green 0.71). Each marker represents a different sonication process. Dashed line represents the best fit linear curve for each treatment.

the correlation coefficient in this case is smaller than that in **Figure 3**. It must be noted that, in six patients with SDR < 0.40, the maximum temperature never exceeded 55°C (see data in the bottom left of **Figure 4**), which agrees with the temperature limit for lesion consolidation. Last, **Figure 4** shows that high temperature rises (>60°C) were achieved even in patients with medium-low SDR values (0.4–0.5), confirming that for SDR values above 0.4, no correlation between the SDR score and the maximum temperature achieved is observed.

To obtain further insights about the relationship between patient- and treatment-related parameters, a Pearson correlation matrix was calculated (**Figure 5**). From this analysis, as mentioned already, a positive significant correlation between SDR and slope of the temperature and energy plots, and between SDR and T_{max}, is evident. However, these three quantities do not significantly correlate with Tx nor with SA and are negatively correlated with the expected FP at the target, thereby confirming that high SDR values allow for the desired temperature with a low total HIFU beam energy delivery to the target. In addition, a positive correlation between SA_s and SA_t was found. Finally, the correlation matrix indicated that SA_t is correlated with Tx_t.

The analysis of intersonication time (S_t), which is highly dependent on the planned energy (because the cooling time of the transducer is automatically calculated in relation to this), is discussed in **Figure S9**. Excluding the inconsistent sonication processes, a total of 1,068 sonication processes were considered. The elapsed temporal periods between the sonication processes were as follows: less than 300 s for 477 times (46.9% of total), <500 s for 746 times (73.4% of total), more than 500 s and <1,000 s for 213 times (21.1% of total), more than 1,000 s and <2,000 s for 54 times (5.3% of total), and more than 2,000 s for three times (0.3% of total).

The analysis of the MR thermometry scanning plane (see **Supplementary Material**) per treatment session has been provided because (in our site) the treating physician found

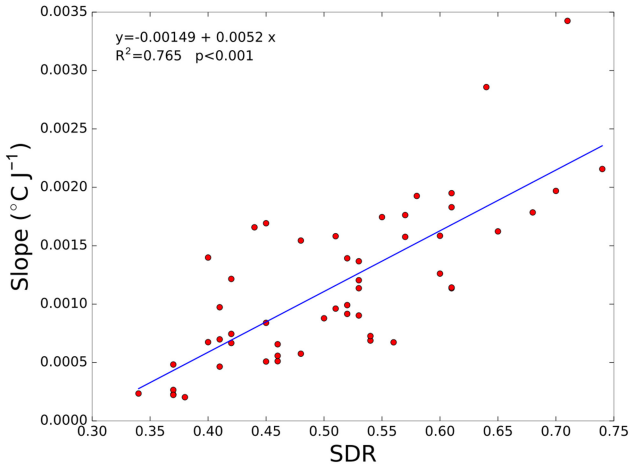

FIGURE 3 | Slope of the temperature vs. energy plot as a function of skull density ratio (SDR) for all of the patients considered. In addition, the best fit linear curve is shown (blue line). Each marker (red circles) represents a patient.

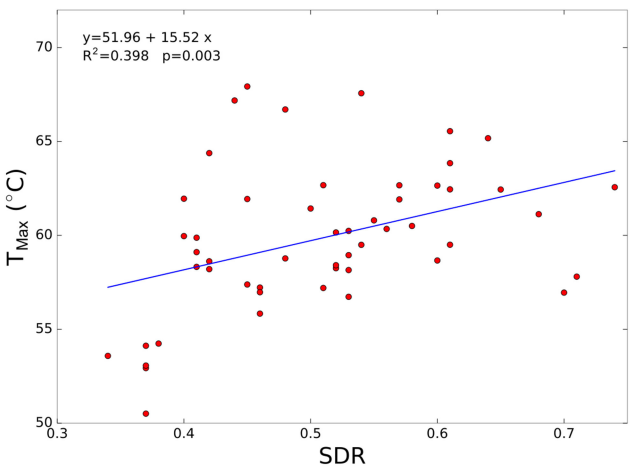

FIGURE 4 | Maximum peak temperature (Tmax) as a function of skull density ratio (SDR) for all enrolled patients. In addition, the best fit linear curve is shown.

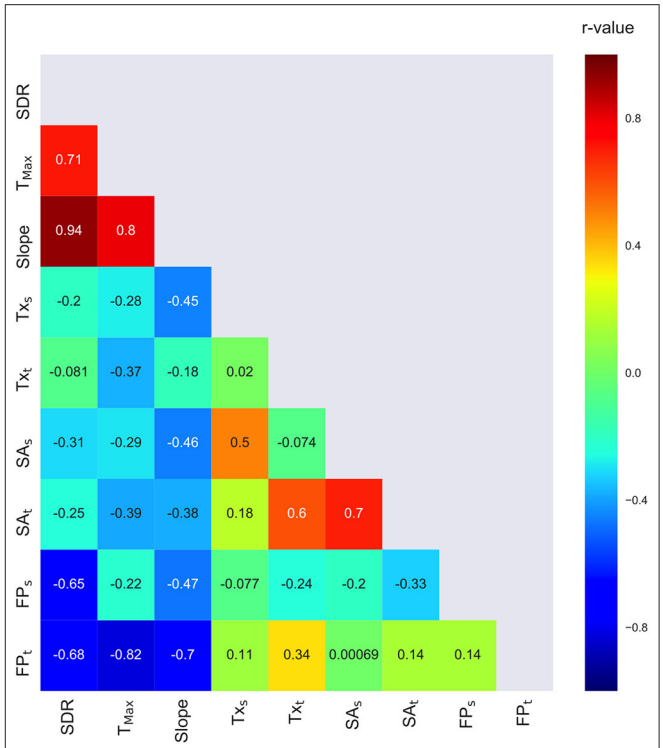

FIGURE 5 | Correlation matrix of patient- and treatment-related data calculated for all patients included in this study.

monitoring the procedure using the axial and the coronal planes—that were, respectively, used for an average of 10.4 (SD ± 3.8) and 7.7 (SD ± 3.0) times, whereas the sagittal plane was used only 2.5 (SD ± 3.0) times per treatment—more reliable. This can be attributed to the average low SNR of the scans obtained in the sagittal plane with the MRI setup used in our facility [15].

DISCUSSION

The main objective of this study was to retrospectively investigate the relationship between the patient- and the treatment-related parameters in a group of patients with ET and PD, who underwent the unilateral thalamotomy procedure of the Vim nucleus for tremor control by a tcMRgFUS system integrated with a 1.5-T MRI unit. The relationship between treatment parameters, consolidated thalamic lesion, and the clinical outcome continue to be areas of investigations [25]. Moreover, to the best of our knowledge, the relationship between patient- and treatment-related technical parameters has been investigated only by Chang et al. on 25 patients [17], of which 15 patients with ET, one with idiopathic PD, and nine with obsessive-compulsive disorder (OCD) were treated with a tcMRgFUS system integrated with a 3-T MRI unit. More recently, the significance of skull bone characteristics in selecting candidates for the FUS procedure was investigated in two groups of patients from a single center (98 patients underwent FUS thalamotomy for ET or PD using a 3-T tcMRgFUS installation and 163 random patients who performed a head CT scan for various clinical indications) [19]. This study concluded that, although low SDR values correlate with high-energy requirement during the FUS procedure, the SDR neither influences the clinical outcome (1 year follow-up) nor provides a good index for prediction. Furthermore, the authors reported that general population SDR sampling does not exhibit any relationship with both sex and age of patients.

In another recent study [18], the influence of skull bone characteristics on the efficacy and safety of procedures performed with a 3-T integrated tcMRgFUS system was investigated using the data of 189 patients with ET collected from five clinical trials conducted in six countries. In addition, this study analyzed a subset of patients with low SDR values and concluded that even if the percentage improvement in tremor rating scale during a 1 year follow-up is not significantly different across the various SDR categories, the probability of reaching a target temperature

of 54°C in patients with SDR < 0.45 is significantly less compared with those with SDR ≥ 0.45.

A study by Jung et al. [20] on five non-embalmed cadaver skulls and 46 patients who underwent tcMRgFUS ablations under 3-T MRI guidance highlighted the SDR, skull volume, and incidence angle of acoustic rays against the skull surface as the most significant factors for a successful energy transmission in a tcMRgFUS procedure.

The results of our study further corroborate the abovementioned results and demonstrate the SDR as the most significant patient-related parameter of all parameters considered in our analysis and can thus influence a tcMRgFUS thalamotomy procedure when a 1.5-T MRI scanner is used. Our study indicates that both the maximum peak temperature in the focal area and the slope of the temperature and energy plots are positively correlated with the SDR. Furthermore, in patients with high SDR values, only a significantly less energy was found to be necessary to attain the temperature for permanent brain lesioning (>50°C) or further consolidate a lesion (>55°C). On the contrary, in patients with low SDR values (<0.40), realizing a temperature rise beyond 50°C was either difficult or impossible. Thus, for patients with SDR < 0.4, treatment could be more difficult even if a significant cumulative thermal dose can be achieved through multiple sonication processes with lower focal temperatures. As reported recently by a study [26], the sonication processes can be repeated to increase the accumulated thermal dose at the target for the cases where attaining a temperature beyond 54°C is impossible (because of patients with unfavorable SDR values or because of reported pain during sonication). A similar approach, but with a totally different objective, has been reported by Gallay et al. [27, 28] for pallidothalamic tractotomy that was successfully achieved in 105 patients by dividing the target region into several subunits with multiple sonication processes with the shortest possible times. This approach could additionally result in increased tolerability of the procedure because high-energy sonication is typically not easily tolerable. However, our analyses confirm that a directly proportional relationship between SDR and energy delivery at the target is not always present. We studied several cases in which a T_{max} exceeding 55°C was easily achieved even in patients with medium-low SDR values (0.4–0.5). Therefore, further analysis on the relationship between SDR and energy delivery (**Figure 2**) on a larger multi-centric data could not only be useful for prospective treatment energy titration optimization but also successfully provide a patient tolerability index and a feasibility score of the procedure. All these results confirm the experimental nature of the FUS procedures performed in the past, and call for further development and optimization in the future.

Even if we never had cases with low SA and Tx elements values (see Materials and Methods), our experience indicates neither the number of transducer elements nor the SA as the discriminating factors for an FUS procedure (see **Table 1** for SA_s, SA_t, Tx_s, and Tx_t values).

However, our study has several limitations. First, we included all of the patients successfully treated at our university hospital without considering the learning curve of both the treating physician and the tcMRgFUS team members (monitoring physician, nurses, radiology technicians, and anesthesiologists). Moreover, this procedure was initially highly experimental, resulting in us facing some challenges and technical snags and/or device malfunctions (see **Table S1**). The initial FUS thalamotomy procedures were usually successfully performed with more than a total of 20 sonication processes, whereas recently, the number was significantly small, occasionally even <10 sonication processes. In addition, a discussion on the duration of the treatment reported in our results is indispensable (see **Figure S9**). For a good estimation of the total treatment, considering an additional 1-h slot is advantageous for patient preparation (elastic membrane positioning, helmet filling, MRI planning scans, procedure planning, and transducer-to-target alignment), intraoperative MRI anatomical scans, and patient discharging times (water drainage from the helmet). However, this procedure time does not include stereotactic frame positioning and removal, which vary greatly based on the tolerability threshold of the patients. Furthermore, starting from September 2017, we upgraded the ExAblate workstation from version 6 to version 7, which introduced the possibility of dynamically modulating each sonication according to the planned energy, transducer power, and sonication duration. Therefore, team expertise and software updates over time could have influenced the execution of the procedures and the process of choosing the most appropriate parameters for each sonication according to the patient-related parameters. Another limitation is that our study included patients with different diseases (ET and PD), although we treated the same target (Vim) in both groups. Nevertheless, a study [17] has reported no statistically significant differences between different diseases (ET, PD, and OCD) and related ablation targets (Vim for ET and PD patients and anterior limb of the internal capsule for OCD patients).

Despite these limitations, this is the first study to investigate the relationship between patient- and treatment-related parameters using a tcMRgFUS system integrated with a 1.5-T MRI unit on a reasonable number of patients from a single center. Furthermore, our study has some novelties: the type of analysis we performed in this study by plotting E_m against SDR, and by plotting the slope of temperature divided by energy delivery against SDR, has not been reported previously in the literature. Although it would be preferable to confirm these results with a multicenter study to compare FUS procedures parameters, thermal monitoring, targeting accuracy, and clinical outcomes from both 1.5-T and 3-T sites, our results appear to be insufficiently highlighting significant differences with respect to the results reported by Chang et al. [17] when an integrated 3-T FUS system is used. Thus, considering the positive effects of using an FUS system integrated with a 1.5-T MRI unit [15], this could facilitate the widespread employment of these devices in the future. We expect the use of dedicated coils with tcMRgFUS systems integrated with 3-T MRI units to bridge this gap in the future. Accordingly, evaluating this aspect will definitely be interesting, specifically for other currently investigated FUS applications in the field of neuroscience, such as brain tumor ablation [12, 29, 30], blood-brain barrier opening [13, 14], and other non-thermal FUS effects [31], in which a much wider

region could be considered for treatment and the ability to attain predefined temperature levels may vary based on the location of the target and the effect to achieve. Lastly, there are currently under investigation MRI-based methods to replicate CT-based measurements of skull properties associated with the success of tcMRgFUS procedures that may deserve attention in the next future [32].

CONCLUSIONS

In the past few years, transcranial MRgFUS has gained great attention in the field of therapeutic brain lesioning, specifically in stereotactic image-guided procedures for neurological disorders. Various studies conducted on patients with movement disorders have reported interesting clinical results that indicate minimal invasiveness and a very low rate of tcMRgFUS procedure-associated risks and adverse events. This retrospective study was conducted to investigate about treatment- and patient-related parameters obtained from FUS procedures performed using a 1.5-T integrated tcMRgFUS system.

The results of this study contribute to extend the knowledge on this topic and confirm the limits and difficulties that may affect an FUS procedure. Our results are in accordance with the data available in the English literature from FUS procedures performed using 3-T integrated tcMRgFUS systems. Thus, this study is beneficial to those operating a tcMRgFUS system, irrespective of the magnetic field strength. Moreover, we expect that the possibility of prospectively setting sonication energy according to the presented curves of energy delivery as a function of SDR for each treatment stage, and importantly updating the reference database with data from numerous cases collected from various treatment facilities across the globe, could lead to further understanding and greater awareness of this emerging technology. The experience we gained in this research indicates that the SDR value still remains one of the most significant technical parameters to be considered for a successful FUS procedure even if is not always correlated to the maximum temperature achievable.

DATA AVAILABILITY STATEMENT

The datasets generated for this study are available on request to the corresponding author.

ETHICS STATEMENT

The studies involving human participants were reviewed and approved by Comitato Etico Palermo 1 (verbale N°4/2018 seduta del 11/04/2018). The patients/participants provided their written informed consent to participate in this study.

AUTHOR CONTRIBUTIONS

CG contributed to the conception and the design of the study. CG and CD'A acquired the data and organized the database. CG and MMa analyzed the data and performed the statistical analysis. CG and MMa wrote the first draft of the manuscript. All the authors contributed to manuscript revision and read and approved the submitted version. Study supervision was done by CG, AN, CC, RL, and MMi.

FUNDING

The installation of the tcMRgFUS equipment used in this study was funded by the Italian Ministry of Education, University and Research (MIUR), within the project Programma Operativo Nazionale 2007–3013 (PONa3_00011; project leader: CC). The research leading to these results received funding from the Italian Ministry of Health Ricerca Finalizzata 2016-Giovani Ricercatori call under grant agreement no. GR-2016-02364526 (principal investigator: CG).

ACKNOWLEDGMENTS

The tcMRgFUS procedures performed at the University Hospital of Palermo were the result of a multidisciplinary collaboration led by the Radiology sections of Palermo and Rome, with essential support from the Neurology Unit and the Neurosurgery Units of the University Hospital of Palermo, and Physicists from the Department of Chemistry and Physics of the University of Palermo. The authors are very grateful for this collaboration.

SUPPLEMENTARY MATERIAL

The Supplementary Material for this article can be found online at: https://www.frontiersin.org/articles/10.3389/fphy.2019.00223/full#supplementary-material

REFERENCES

1. Anzidei M, Napoli A, Sandolo F, Marincola BC, Di Martino M, Berloco P, et al. Magnetic resonance-guided focused ultrasound ablation in abdominal moving organs: a feasibility study in selected cases of pancreatic and liver cancer. *Cardiovasc Intervent Radiol.* (2014) **37**:1611–7. doi: 10.1007/s00270-014-0861-x
2. Clement GT, Hynynen K. A non-invasive method for focusing ultrasound through the human skull. *Phys Med Biol.* (2002) **47**:1219–36. doi: 10.1088/0031-9155/47/8/301
3. Miocinovic S, Somayajula S, Chitnis S, Vitek JL. History, applications, and mechanisms of deep brain stimulation. *JAMA Neurol.* (2013) **70**:163–71. doi: 10.1001/2013.jamaneurol.45
4. Dallapiazza RF, Lee DJ, De Vloo P, Fomenko A, Hamani C, Hodaie M, et al. Outcomes from stereotactic surgery for essential tremor. *J Neurol Neurosurg Psychiatr.* (2019) **90**:474–82. doi: 10.1136/jnnp-2018-318240
5. Rohani M, Fasano A. Focused ultrasound for essential tremor: review of the evidence and discussion of current hurdles. *Tremor Other Hyperkinet Mov.* (2017) **7**:462. doi: 10.7916/D8Z89JN1
6. Elias WJ, Lipsman N, Ondo WG, Ghanouni P, Kim YG, Lee W, et al. A randomized trial of focused ultrasound thalamotomy for essential tremor. *N Engl J Med.* (2016) **375**:730–9. doi: 10.1056/NEJMoa1600159
7. Schlesinger I, Eran A, Sinai A, Erikh I, Nassar M, Goldsher D, et al. MRI guided focused ultrasound thalamotomy for moderate-to-severe tremor in Parkinson's disease. *Parkinsons Dis.* (2015) **2015**:219149. doi: 10.1155/2015/219149

8. Sperling SA, Shah BB, Barrett MJ, Bond AE, Huss DS, Gonzalez Mejia JA, et al. Focused ultrasound thalamotomy in Parkinson disease. Nonmotor outcomes and quality of life. *Neurology.* (2018) **91**:e1275–84. doi: 10.1212/WNL.0000000000006279
9. Zaaroor M, Sinai A, Goldsher D, Eran A, Nassar M, Schlesinger I. Magnetic resonance-guided focused ultrasound thalamotomy for tremor: a report of 30 Parkinson's disease and essential tremor cases. *J Neurosurg.* (2018) **128**:202–10. doi: 10.3171/2016.10.JNS16758
10. Jeanmonod D, Werner B, Morel A, Michels L, Zadicario E, Schiff G, et al. Transcranial magnetic resonance imaging-guided focused ultrasound: noninvasive central lateral thalamotomy for chronic neuropathic pain. *Neurosurg Focus.* (2012) **32**:E1. doi: 10.3171/2011.10.FOCUS11248
11. Jung HH, Chang WS, Rachmilevitch I, Tlusty T, Zadicario E, Chang JW. Different magnetic resonance imaging patterns after transcranial magnetic resonance-guided focused ultrasound of the ventral intermediate nucleus of the thalamus and anterior limb of the internal capsule in patients with essential tremor or obsessive-compulsive disorder. *J Neurosurg.* (2015) **122**:162–8. doi: 10.3171/2014.8.JNS132603
12. Grasso G, Midiri M, Catalano C, Gagliardo C. Transcranial magnetic resonance-guided focused ultrasound surgery for brain tumor ablation: are we ready for this challenging treatment? *World Neurosurg.* (2018) **119**:438–40. doi: 10.1016/j.wneu.2018.09.017
13. Lipsman N, Meng Y, Bethune AJ, Huang Y, Lam B, Masellis M, et al. Blood-brain barrier opening in Alzheimer's disease using MR-guided focused ultrasound. *Nat Commun.* (2018) **9**:2336. doi: 10.1038/s41467-018-04529-6
14. Mainprize T, Lipsman N, Huang Y, Meng Y, Bethune A, Ironside S, et al. Blood-brain barrier opening in primary brain tumors with non-invasive mr-guided focused ultrasound: a clinical safety and feasibility study. *Sci Rep.* (2019) **9**:321. doi: 10.1038/s41598-018-36340-0
15. Gagliardo C, Midiri M, Cannella R, Napoli A, Wragg P, Collura G, et al. Transcranial magnetic resonance-guided focused ultrasound surgery at 1.5T: a technical note. *Neuroradiol J.* (2019) **32**:132–8. doi: 10.1177/1971400918818743
16. Iacopino DG, Gagliardo C, Giugno A, Giammalva GR, Napoli A, Maugeri R, et al. Preliminary experience with a transcranial magnetic resonance-guided focused ultrasound surgery system integrated with a 1.5-T MRI unit in a series of patients with essential tremor and Parkinson's disease. *Neurosurg Focus.* (2018) **44**:E7. doi: 10.3171/2017.11.FOCUS17614
17. Chang WS, Jung HH, Zadicario E, Rachmilevitch I, Tlusty T, Vitek S, et al. Factors associated with successful magnetic resonance-guided focused ultrasound treatment: efficiency of acoustic energy delivery through the skull. *J Neurosurg.* (2016) **124**:411–6. doi: 10.3171/2015.3.JNS142592
18. D'Souza M, Chen KS, Rosenberg J, Elias WJ, Eisenberg HM, Gwinn R, et al. Impact of skull density ratio on efficacy and safety of magnetic resonance-guided focused ultrasound treatment of essential tremor. *J Neurosurg.* (2019). doi: 10.3171/2019.2.JNS183517. [Epub ahead of print].
19. Boutet A, Gwun D, Gramer R, Ranjan M, Elias GJB, Tilden D, et al. The relevance of skull density ratio in selecting candidates for transcranial MR-guided focused ultrasound. *J Neurosurg.* (2019). doi: 10.3171/2019.2.JNS182571. [Epub ahead of print].
20. Jung NY, Rachmilevitch I, Sibiger O, Amar T, Zadicario E, Chang JW. Factors related to successful energy transmission of focused ultrasound through a skull : a study in human cadavers and its comparison with clinical experiences. *J Kor Neurosurg Soc.* (2019) **62**:712–22. doi: 10.3340/jkns.2018.0226
21. Ghanouni P, Pauly KB, Elias WJ, Henderson J, Sheehan J, Monteith S, et al. Transcranial MRI-guided focused ultrasound: a review of the technologic and neurologic applications. *Am J Roentgenol.* (2015) **205**:150–9. doi: 10.2214/AJR.14.13632
22. Oliphant TE. Python for scientific computing. *Comput Sci Engg.* (2007) **9**:10–20. doi: 10.1109/MCSE.2007.58
23. The Sage D. *"SageMath, The Sage Mathematics Software System (Version 7.5.1)"*. The Sage Developers (2017).
24. Valentino F, Cosentino G, Maugeri R, Giammalva R, Iacopino GD, Marrale M, et al. Is transcranial magnetic resonance imaging-guided focused ultrasound a repeatable treatment option? Case report of a retreated patient with tremor combined with parkinsonism. *Oper Neurosurg.* (2019). doi: 10.1093/ons/opz300. [Epub ahead of print].
25. Huang Y, Lipsman N, Schwartz ML, Krishna V, Sammartino F, Lozano AM, et al. Predicting lesion size by accumulated thermal dose in MR-guided focused ultrasound for essential tremor. *Med Phys.* (2018) **45**:4704–10. doi: 10.1002/mp.13126
26. Jones RM, Kamps S, Huang Y, Scantlebury N, Lipsman N, Schwartz ML, et al. Accumulated thermal dose in MRI-guided focused ultrasound for essential tremor: repeated sonications with low focal temperatures. *J Neurosurg.* (2019). doi: 10.3171/2019.2.JNS182995. [Epub ahead of print].
27. Gallay MN, Moser D, Jeanmonod D. Safety and accuracy of incisionless transcranial MR-guided focused ultrasound functional neurosurgery: single-center experience with 253 targets in 180 treatments. *J Neurosurg.* (2019). doi: 10.3171/2017.12.JNS172054. [Epub ahead of print].
28. Gallay MN, Moser D, Federau C, Jeanmonod D. Anatomical and technical reappraisal of the pallidothalamic tractotomy with the incisionless transcranial MR-guided focused ultrasound. A Technical Note. *Front Surg.* (2019) **6**:2. doi: 10.3389/fsurg.2019.00002
29. McDannold N, Clement GT, Black P, Jolesz F, Hynynen K. Transcranial magnetic resonance imaging- guided focused ultrasound surgery of brain tumors: initial findings in 3 patients. *Neurosurgery.* (2010) **66**:323–32. doi: 10.1227/01.NEU.0000360379.95800.2F
30. Coluccia D, Fandino J, Schwyzer L, O'Gorman R, Remonda L, Anon J, et al. First noninvasive thermal ablation of a brain tumor with MR-guided focused ultrasound. *J Ther Ultrasound.* (2014) **2**:17. doi: 10.1186/2050-5736-2-17
31. Prada F, Kalani MYS, Yagmurlu K, Norat P, Del Bene M, DiMeco F, et al. Applications of focused ultrasound in cerebrovascular diseases and brain tumors. *Neurotherapeutics.* (2019) **16**:67–87. doi: 10.1007/s13311-018-00683-3
32. Caballero-Insaurriaga J, Rodriguez-Rojas R, Martinez-Fernandez R, Del-Alamo M, Diaz-Jimenez L, Avila M, et al. Zero TE MRI applications to transcranial MR-guided focused ultrasound: patient screening and treatment efficiency estimation. *J Magn Reson Imaging.* (2019) **50**:1583–92. doi: 10.1002/jmri.26746

Conflict of Interest: The authors declare that the research was conducted in the absence of any commercial or financial relationships that could be construed as a potential conflict of interest.